Available online at www.sciencedirect.com
ScienceDirect
Precambrian Research 159 (2007) 260–274
Precambrian Research
www.elsevier.com/locate/precamres

Trace element and Nd-isotopic evidence for sediment sources in the mid-Proterozoic Vindhyan Basin, central India

Ramananda Chakrabarti [a,1], Asish R. Basu [a,*], Amitabha Chakrabarti [b]

[a] *Department of Earth and Environmental Sciences, University of Rochester, Rochester, NY 14627, USA*
[b] *Department of Geology and Geophysics, Indian Institute of Technology Kharagpur, Kharagpur 721302, India*

Received 28 November 2006; received in revised form 26 June 2007; accepted 4 July 2007

Abstract

Ancient sediments reflect the compositions of old eroded continental crustal material and preserve geochemical signatures of paleo-tectonic and volcanic events. Geochemical study of such sediments provides insight into tectonic events that shaped the face of the Earth. Nd isotopes are best suited for such studies because rare earth elements (REE), specifically Sm and Nd are not fractionated during post-depositional processes such as erosion, transportation and diagenesis of organic-poor sediments and hence reflect the source composition of these sediments. Sedimentation in the Proterozoic Vindhyan Basin of central India with a ∼4 km thick succession of unmetamorphosed and mostly undeformed sediments lasted over 1000 Ma from ∼1630 Ma up to the Precambrian–Cambrian boundary. These sediments provide an ideal opportunity to study the evolution of ancient continental crust as well as the tectonic evolution of Peninsular India.

The occurrence of porcellanites in the lower part of the basin indicates active volcanism during deposition of the Vindhyan sediments. These tuffs show large ion lithophile element (LILE) enrichment as well as depletions in Nb and Ta in primitive mantle-normalized plots, characteristic of an arc volcanic source. In combined trace element ratio plots, these volcanic rocks indicate mixing between mantle-derived melts and the continental crust and overlap with the composition of global arcs. Their initial ε_{Nd} at 1630 Ma, ranging from −5.7 to −0.9, is similar to those observed in 'Andean-type' continental margin arcs.

Trace element concentration patterns as well as Nd isotopic compositions of the clastic and non-clastic sediments of the Vindhyan Basin, from one of the type-localities of the Vindhyan stratigraphy in the Son valley, are vastly different from those of the Bundelkhand granite, which is the basement for these sediments, indicating that these granitic rocks were not a major source of sediments for the Vindhyan Basin. Our Nd isotopic study clearly indicates that sedimentation in the Vindhyan Basin, which lasted over ∼1 Ga, was not continuous. The boundaries between the Semri and Kaimur Groups as well as the Rewa and Bhander Groups are characterized by abrupt changes in the Nd isotopic compositions indicating changes in provenance, with sediments in the Kaimur and Bhander Groups being derived from more juvenile sources compared to the Semri and Rewa Groups, respectively. This inference is also supported by changes in T_{DM} and $f_{Sm/Nd}$ for the sediments across these boundaries. The strikingly different trace element patterns of the Rewa Group sediments compared to the underlying Kaimur sediments indicates that sediment sources also changed across the Kaimur–Rewa boundary. Multiple changes in provenance in the Vindhyan sediments indicate that this basin was tectonically active during the entire span of sedimentation.

While there is some uncertainty in determining the exact sources of sediments for the Vindhyan Basin, we argue on the basis of our geochemical, in particular Nd-isotopic ratios data, and available paleocurrent data that majority of the sediments were derived

* Corresponding author. Fax: +1 585 244 5689.
E-mail address: abasu@earth.rochester.edu (A.R. Basu).
[1] Present address: Department of Earth and Planetary Sciences, Harvard University, Cambridge, MA 02138, USA.

0301-9268/$ – see front matter
doi:10.1016/j.precamres.2007.07.003

from a now-extinct Andean-type arc source in the south that resulted from a southerly dipping subduction prior to the collision of the Bhandara and Bundelkhand cratons. According to this reconstruction, the Vindhyan Basin was initiated as a foreland Basin after the collision of these two cratons.

Keywords: Trace elements; Nd-isotope; Provenance; Vindhyan sedimentary Basin; Andean-type arc

1. Introduction

Ancient sedimentary records preserve the chemical characteristics of old continental crust. Studying these sediments is critical to our understanding of the evolution of the crust through time. In addition, chemical and isotopic signatures of tectono-volcanic events are often preserved in these sedimentary records, which reflect those of their source rocks. Nd isotopes are a good indicator of sediment provenance (Miller and O'Nions, 1984; Nelson and DePaolo, 1988; Basu et al., 1990; Gleason et al., 1994; Simien et al., 1999), and are particularly useful for fine-grained sediments for which it is generally impossible to determine the provenance petrographically. Rare earth elements (REE) including Sm and Nd are not fractionated during surficial processes such as erosion, transportation and diagenesis, except for organic-rich sediments (e.g. Hannigan and Basu, 1998; Chakrabarti et al., 2007 and references therein). Hence, for organic-poor sediments the REE concentrations and Nd isotopic compositions of sediments reflect those of the source material. In addition, depleted mantle Nd model ages (T_{DM}) add a temporal dimension to the provenance study of sediments by providing extraction ages of the sediment sources from the depleted mantle. Sm–Nd analyses of fine-grained clastic sediments are also a powerful sedimentological tool to elucidate paleogeography, sediment recycling and maturity as well as aspects of sediment transport (Miller and O'Nions, 1984).

The Proterozoic Vindhyan Basin of central India (Fig. 1), with a ∼4 km thickness (Bhattacharyya, 1996) of unmetamorphosed sediments provides an ideal opportunity to study the evolution of ancient continental crust. The Vindhyan Supergroup preserves the thickest Precambrian sedimentary succession in India. Age estimates indicate that the initiation of sedimentation took place as early as 1721 Ma (Ray, 2006) while the youngest sediments extend up to the Precambrian–Cambrian boundary (Chakrabarti, 1990). This duration of sedimentation, if continuous, is certainly among the longest in the world. In addition, the Vindhyan rocks have been hosts for interesting but controversial fossil discoveries, including recent reports of triploblastic trace fossils (Seilacher et al., 1998) from the mid-Proterozoic lower sedimentary units of the basin. Given the vastness of this basin with an area of ∼178,000 km^2 (Tandon et al., 1991) as well as the supposedly long duration of sedimentation, this basin provides unique opportunities for paleo-tectonic reconstructions and sediment-source determinations, along with inferences on climate stability during sediment deposition in the mid-Proterozoic.

We present here a comprehensive trace element and Nd isotopic study of the Vindhyan Basin sediments in central India, a major mid-Proterozoic continental sedimentary succession in the world. The goal of this study is to utilize the trace element and Nd-isotopic composition of the sediments to understand the sedimentation history of the basin in light of their source rock characteristics. This combined trace element and Nd-isotopic study has implications for the genesis of the rhyolite tuff (porcellanite) layers in the lower part of the basin in petro-tectonic terms, provenance of the clastic and non-clastic sediments, as well as for the tectonic evolution of this large basin.

2. Geologic setting and sample description

The Vindhyan Basin (Fig. 1) with an area of 178,000 km^2 (Tandon et al., 1991) is one of the largest Proterozoic basins of the world and comprises a ∼4 km thick sequence of mostly undeformed and unmetamorphosed sediments, dominantly immature, siliciclastic in the lower part succeeded by more carbonate rich sediments towards the top. The Vindhyan Basin is bordered by the Aravalli–Delhi orogenic belt (2500–900 Ma) (Roy, 1988) in the west while the Satpura orogenic belt (1600–850 Ma) (Verma, 1991) occurs to the south and east. The Bundelkhand granite massif (3.3–2.5 Ga) (Crawford and Compston, 1970; Mondal et al., 2002) occurring at the center of the basin divides the basin into two sub-basins—the Son Valley Vindhyans to the east and the Aravalli–Vindhyans to the west. Much of the northern part of the Vindhyan Basin along with the Aravalli–Delhi fold belt and the Bundelkhand granite-gneiss is overlain by recent alluvium of the Gangetic plain while the southern part of the Vindhyan Basin

is covered by the Deccan Trap lava (Cretaceous to Oligocene) (Krishnan, 1968). Along the southern edge of the Vindhyan Basin and along the eastern edge of the Bundelkhand granite-gneiss complex occurs a low-grade metamorphic Group of volcano-sedimentary rocks, known as the Mahakoshal Group (2400 Ma) and the Bijawar Group (2100 Ma), respectively (Das et al., 1990; Roy and Bandyopadhyay, 1990).

The southern edge of the Vindhyan Basin is also marked by a major structural feature called the Narmada-Son lineament (Fig. 1) which is considered to have formed along Archean structural trends and remained active throughout its geologic history up to the present (Naqvi and Rogers, 1987; Kaila et al., 1989). South of this lineament, a southerly dipping reverse fault separates the Vindhyan Supergroup rocks from the Satpura belt in the Son valley (Tewari, 1968). This faulting caused deformation of the Vindhyan sedimentary rocks exposed immediately to the north but cannot be traced farther west, as it is possibly covered by younger structures (Rogers, 1986). The western margin of the Vindhyan Basin is marked by the Great Boundary Fault, another major lineament, characterized by westerly dipping faults, which separates the Vindhyans from the Aravalli–Delhi fold belt rocks (Fig. 1).

A composite stratigraphic section of the Vindhyan Supergroup of rocks is shown in Fig. 2. The samples of the present study were collected from the Son valley Vindhyans, which is broadly divided into four groups—Semri, Kaimur, Rewa and Bhander, from the bottom to the top (Fig. 2). The Semri Group is also called the lower Vindhyans while the Kaimur, Rewa and Bhander Groups comprise the upper Vindhyan rocks. The only volcanic unit is the Porcellanite Formation (rhyolite tuffs) exposed in the lower part of the Vindhyans (Fig. 2). Recent studies, however, indicate presence of thin and laterally discontinuous volcanoclastic layers, dominantly of intermediate compositions, at the base of the Kaimur Group and at different stratigraphic levels within the Rewa Group of rocks (Chakraborty et al., 1996). The samples collected for the present study (Fig. 2) are primarily sandstones and limestones from all the four groups, and they include from bottom to top, the Churhat Sandstone, Rhotas Limestone, lower Kaimur Sandstone, upper Rewa Sandstone, Bhander Limestone (impure), lower Bhander Sandstone and the Sirbu Shale, respectively. We also selected a sample of the Bundelkhand granite, the basement rock for this basin, as well as several samples of porcellanites from a supposedly laterally continuous layer of this key horizon.

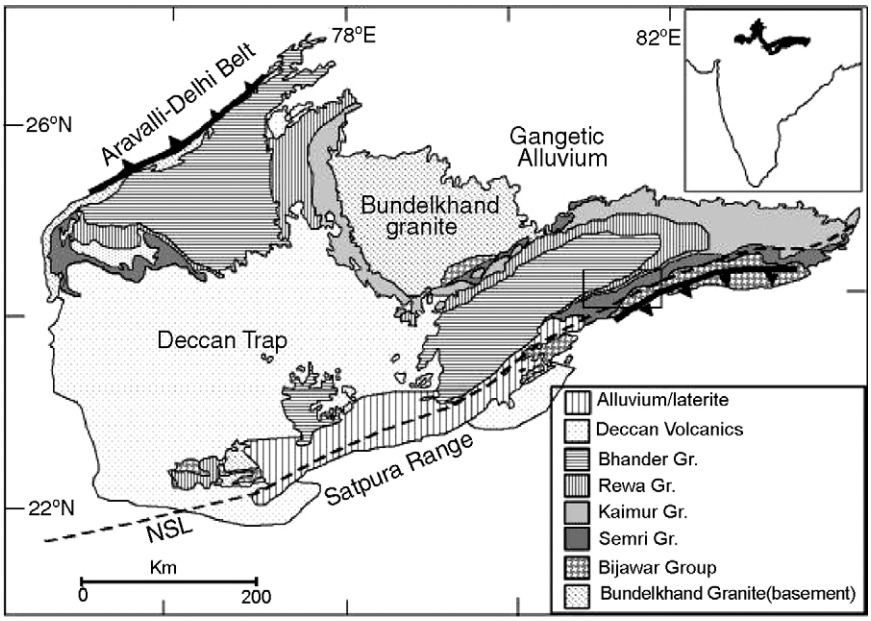

Fig. 1. Simplified geological map of the Proterozoic Vindhyan Basin of central India. Also shown are the locations of the Deccan Traps, Bundelkhand granite, Satpura Range, Gangetic alluvium and the Aravalli–Delhi belt. The dashed line is the Narmada-Son lineament (NSL). Prominent westerly and southerly dipping thrust faults are also shown from the literature (see text for details). Samples for the present study were collected from the region marked with a rectangle in the eastern half of the Vindhyan Basin, traditionally known as the Son valley Vindhyans, and include prominent lithostratigraphic units from the four groups of the Vindhyan Basin. In selecting these samples, the primary purpose was a vertical chronostratigraphic representation (see Fig. 2) of the entire basin as exposed in the southern part of the basin.

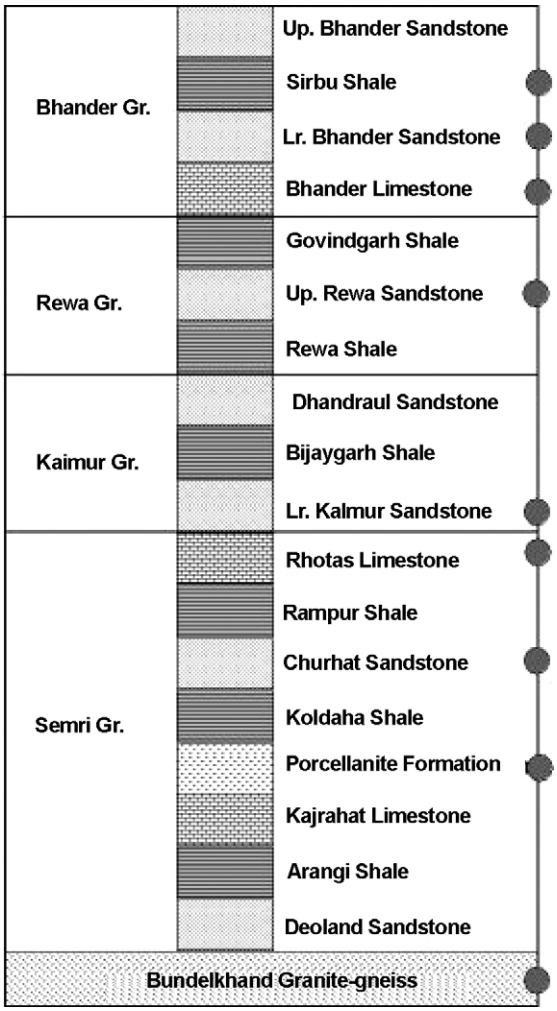

Fig. 2. Simplified stratigraphy (after Chakraborty, 2006) of the Son valley section of the Vindhyan Basin, showing the four Groups viz. Semri, Kaimur, Rewa and Bhander from bottom to top, respectively. The thicknesses of the units are not to scale. The Bundelkhand Granite-gneiss is the basement of the Vindhyan Basin. Also shown with shaded circles are the lithounits from which samples were analyzed for the present study. The total thickness of sediments from the bottom to the top of this section is approximately 4 km (Bhattacharyya, 1996).

3. Analytical methods

Thirty-one samples, including samples of the basement Bundelkhand granite, rhyolite tuff samples from the Porcellanite Formation, sandstones, and limestones from different stratigraphic horizons of the Vindhyan Basin were analyzed for trace element concentrations and Nd-isotope ratios. Ten samples of the Rhotas Limestone were also analyzed for their Pb-isotopic composition. Large-size whole rock samples were crushed for geochemical and isotopic analyses. Trace element concentrations were determined using an inductively coupled plasma mass spectrometer (ICP-MS, Thermo Elemental, X-7) while the radiogenic isotopic ratios were measured with a thermal ionization mass spectrometer (TIMS, VG Sector), both at the University of Rochester.

For ICPMS analyses in our laboratory, 25–50 mg powder of whole rock samples were treated with mixtures of HF and HNO_3 acids and diluted to 100 ml in 2% HNO_3 solution with ~10 ppb internal standard of In, Cs, Re, and Bi. Table 1

shows the elemental concentrations of the samples obtained by using BCR-2 and AGV-2 (concentrations from USGS) as known external standards. The concentrations of the various elements, other than the rare earth elements, are within 5% error, as estimated from repeated measurements of SRM 278 (obsidian-NIST), BHVO-2 (basalt-USGS) and G-1 (granite-USGS) rock standards, which were run as unknowns. The rare earth elements, in particular Sm and Nd, are more precisely determined to within 2% error.

For isotopic measurements, 100–200 mg of powdered whole rock samples were dissolved in HF–HNO_3 and HCl acids followed by chromatographic separation of Nd and Pb. Nd-isotopes were measured using the procedures established for our laboratory at the University of Rochester (Basu et al., 1990). Pb isotopes were also measured in our laboratory using the silica-gel technique by TIMS (Sharma et al., 1992). Filament temperature during Pb-isotope ratio measurements was monitored continuously and raw ratios were calculated as weighted averages of the ratios measured at 1150, 1200, and 1250 °C, respectively. The reported Pb-isotopic data were corrected for mass fractionation of $0.12 \pm 0.03\%$ per amu based on replicate analyses of the NBS-982 Equal Atom Pb Standard measured in the same fashion. Our laboratory procedural blanks were less than 200 pg for both Nd and Pb. No blank correction was necessary for the data.

4. Age of sedimentation and Pb-isotopic data

The best age constraints for the time of sedimentation of the Vindhyan Basin are obtained from the Porcellanite Formation (also known as the Deonar Formation) of the lowermost Semri Group. Recent U-Pb zircon ages (Rasmussen et al., 2002; Ray et al., 2002) indicate that the age of these rhyolite tuffs are ~1631 Ma. Tuffs from within the overlying Rampur Shale (Fig. 2) give ages of ~1599 Ma indicating that the Churhat Sandstone was deposited between 1628 ± 8 Ma and 1599 ± 8 Ma. Pb–Pb ages for the Rhotas Formation, the uppermost unit of the Semri Group, range from 1601 ± 130 Ma (Ray et

Table 1
Trace element concentrations of the Vindhyan basin rocks. Concentrations are shown in μg/g (ppm) and were determined by ICPMS at the University of Rochester

Sample#	Description	Rb	Sr	Y	Zr	Nb	Ta	Ba	La	Ce	Pr	Nd	Sm	Eu	Gd	Tb	Dy
Sirbu-1	Sirbu Shale	60	31.7	23.4	85.2	7.9	0.67	281	17.1	34.4	3.80	16.9	4.16	0.89	5.1	0.74	4.05
LBS-1	Lr Bhander Sst	53	29.2	12.5	208	5.8	0.48	164	16.4	32.7	3.84	14.9	3.12	0.51	2.52	0.40	2.28
LBS-2		46.8	90.8	15.1	282	7.4	0.60	203	20.8	41.7	4.88	19.0	4.14	0.62	3.27	0.50	2.74
LBS-3		28.4	23.5	15.7	420	6.7	0.51	159	18.1	37.5	4.23	16.4	3.69	0.54	3.08	0.50	2.88
LBS-4		68	34.1	27.8	479	10.3	0.90	316	31.9	66	7.7	30.0	6.9	1.04	5.7	0.87	5.3
LBL-1	Bhander Lst	18.5	191	5.1	21.0	1.62	0.12	51	5.1	10.8	1.26	5.0	1.03	0.20	0.92	0.15	0.87
LBL-2		64	47.4	19.5	53.7	4.49	0.35	1229	20.0	48.0	4.84	18.6	3.82	0.67	3.74	0.57	3.33
LBL-3		48.5	153	13.5	78.7	4.87	0.38	94	13.4	28.1	3.22	12.5	2.64	0.46	2.33	0.38	2.30
VR-1	Rewa Sst	1.41	10.4	3.94	20.4	0.48	0.05	6.3	6.3	14.1	1.54	5.5	1.06	0.16	0.80	0.12	0.69
VR-2		1.21	8.4	3.22	17.6	0.38	0.04	6.0	5.4	12.2	1.30	4.84	0.92	0.14	0.68	0.10	0.58
AC-KMS1	Kaimur Sst	47.1	27.8	25.2	460	12.0	1.08	174	22.2	43.8	5.1	19.3	4.27	0.74	4.16	0.74	4.33
VK-1		80	19.5	11.2	111	4.16	0.34	227	12.7	22.5	3.10	11.5	2.43	0.47	2.14	0.33	1.86
VK-2		55	15.0	7.7	104	4.14	0.32	179	8.8	17.6	2.09	7.5	1.50	0.29	1.38	0.22	1.30
VK-3		46.8	34.2	9.2	104	5.6	0.44	69	17.6	36.2	4.01	13.7	2.51	0.44	1.89	0.27	1.60
VK-3A		2.59	20.1	5.1	45.3	1.34	0.12	14.8	9.0	19.8	2.31	8.4	1.64	0.25	1.15	0.17	0.90
VRH-2-1	Rhotas Lst	86	87	9.3	44.9	4.63	0.38	92	4.30	8.4	1.09	4.25	0.96	0.19	0.96	0.16	1.01
VRH-2		74	85	7.9	38.3	4.08	0.34	79	4.33	8.4	1.09	4.18	0.92	0.18	0.90	0.14	0.89
VRH-1		36.5	149	6.2	20.0	2.17	0.18	43.7	4.81	8.4	1.10	3.99	0.80	0.15	0.75	0.11	0.71
CHAC-2	Churhat Sst	40.0	12.3	7.2	59	2.16	0.19	159	10.4	26.4	3.7	14.8	2.73	0.46	1.68	0.22	1.23
CHAC-1		212	46.1	25.7	142	10.4	0.86	338	27.1	61	6.2	22.7	4.75	0.94	4.09	0.66	4.60
Porac1	Porcellanite	225	21.5	33.2	163	16.2	1.44	653	71	104	15.5	54	10.4	1.09	8.2	1.16	6.0
Porac2		165	14.9	21.3	95	9.9	0.79	596	41.7	72	9.2	34.2	6.6	0.74	5.3	0.77	4.13
Porac3		65	94	29.3	118	12.1	0.62	423	92	174	19.9	68.	12.6	1.75	9.3	1.13	5.4
Porac4		420	30.0	44.3	158	17.1	1.53	3148	68	123	15.1	51	9.1	1.02	6.9	1.07	6.4
Porac5		474	34.6	51.4	175	20.2	1.71	2940	74	173	16.01	54	9.8	1.10	7.8	1.19	7.3
Porac6		120	8.1	33.2	96	10.2	0.99	562	45.5	96	12.0	43.3	8.5	0.95	6.5	0.96	5.4
Porac7		221	9.8	22.8	96	10.9	0.99	678	51	93	11.0	37.6	6.8	0.80	4.72	0.65	3.67
Porac8		285	27.3	34.0	207	20.4	1.81	791	72	136	15.3	52	9.7	0.92	7.4	1.06	5.7
Porac9		209	22.4	41.2	154	15.6	1.45	627	63	120	13.7	47.9	9.4	1.00	8.1	1.24	7.0
Porac10		85	97	20.6	124	7.9	0.96	343	23.5	49.0	5.7	21.3	4.56	0.66	4.10	0.59	3.30
AC-BG1	Bundelkhand Gr.	297	117	8.3	79.0	5.9	1.04	1477	15.5	27.2	2.81	9.4	1.28	0.34	1.29	0.21	1.25

Table 1 (*Continued*)

Sample#	Description	Ho	Er	Tm	Yb	Lu	Hf	Ta	Pb	Th	U	$La/Yb_{(N)}$	Eu/Eu*	Ce/Pb	Nb/Ta	Zr/Sm
Sirbu-1	Sirbu Shale	0.81	2.11	0.31	1.96	0.28	2.39	0.67	14.9	8.5	1.63	5.9	0.15	2.30	11.8	20.5
LBS-1	Lr Bhander Sst	0.46	1.28	0.18	1.50	0.23	6.0	0.48	7.4	8.0	2.05	7.4	0.13	4.40	11.9	66.5
LBS-2		0.53	1.49	0.21	1.69	0.27	8.2	0.60	10.7	12.4	2.61	8.3	0.13	3.90	12.5	68.0
LBS-3		0.57	1.73	0.25	2.10	0.33	12.5	0.51	5.8	10.5	2.47	5.8	0.13	6.4	13.3	114.0
LBS-4		1.02	2.93	0.41	3.35	0.52	15.0	0.90	17.4	22.3	4.57	6.4	0.13	3.76	11.5	69.6
LBL-1	Bhander Lst	0.17	0.48	0.06	0.47	0.07	0.58	0.12	4.51	2.07	0.43	7.4	0.13	2.39	13.7	20.3
LBL-2		0.63	1.63	0.20	1.47	0.22	1.36	0.35	15.2	6.1	2.02	9.2	0.13	3.15	12.8	14.1
LBL-3		0.47	1.30	0.17	1.36	0.20	2.20	0.38	10.4	6.6	1.09	6.7	0.13	2.70	12.9	29.8
VR-1	Rewa Sst	0.14	0.37	0.05	0.33	0.05	0.55	0.05	8.9	1.67	0.36	12.7	0.15	1.57	8.8	19.3
VR-2		0.11	0.31	0.04	0.29	0.04	0.48	0.04	7.2	1.41	0.31	12.7	0.15	1.70	9.9	19.2
AC-KMS1	Kaimur Sst	0.87	2.46	0.33	2.65	0.41	13.6	1.08	10.5	11.4	2.07	5.7	0.13	4.19	11.1	107.7
VK-1		0.39	1.11	0.18	1.22	0.18	2.99	0.34	8.3	5.2	0.99	7.1	0.15	2.72	12.4	45.9
VK-2		0.28	0.79	0.13	0.88	0.13	2.81	0.32	6.3	3.92	1.01	6.8	0.15	2.79	12.8	69.4
VK-3		0.35	1.06	0.18	1.29	0.19	2.83	0.44	2.14	6.6	1.51	9.2	0.15	16.9	12.8	41.6
VK-3A		0.18	0.49	0.08	0.51	0.07	1.29	0.12	58.2	3.61	1.32	12.0	0.15	0.34	11.2	27.6
VRH-2-1	Rhotas Lst	0.24	0.72	0.12	0.80	0.12	1.16	0.38	5.4	5.00	1.51	3.61	0.15	1.54	12.2	46.7
VRH-2		0.21	0.61	0.10	0.68	0.10	1.01	0.34	4.48	4.50	1.44	4.33	0.15	1.87	12.2	41.5
VRH-1		0.16	0.46	0.07	0.48	0.07	0.50	0.18	2.37	2.41	0.85	6.8	0.15	3.54	11.9	24.9
CHAC-2	Churhat Sst	0.25	0.68	0.09	0.70	0.11	1.67	0.19	3.62	4.70	1.05	9.9	0.13	7.3	11.6	21.6
CHAC-1		0.94	2.73	0.38	2.98	0.46	4.31	0.86	11.6	18.3	3.60	6.1	0.13	5.2	12.1	29.8
Porac1	Porcellanite	1.18	3.22	0.50	3.41	0.49	4.91	1.44	23.6	32.6	5.8	14.0	0.15	4.43	11.3	15.7
Porac2		0.77	2.06	0.27	2.14	0.33	3.10	0.79	23.3	16.6	3.35	13.2	0.13	3.08	12.5	14.4
Porac3		1.00	2.66	0.40	2.66	0.38	3.03	0.62	20.6	11.7	3.37	23.3	0.15	8.5	19.6	9.4
Porac4		1.45	4.21	0.69	4.72	0.72	4.82	1.53	6.0	27.6	5.9	9.8	0.15	20.6	11.2	17.3
Porac5		1.67	4.96	0.81	5.6	0.85	5.46	1.71	11.4	36.1	6.8	8.9	0.15	15.1	11.8	17.9
Porac6		1.14	3.17	0.49	3.26	0.47	3.12	0.99	8.5	17.5	3.49	9.4	0.15	11.3	10.3	11.3
Porac7		0.80	2.38	0.39	2.73	0.40	3.05	0.99	5.0	20.7	2.85	12.5	0.15	18.6	11.0	14.2
Porac8		1.18	3.36	0.54	3.73	0.54	5.9	1.81	18.1	37.5	6.0	13.0	0.15	7.5	11.3	21.4
Porac9		1.46	4.03	0.63	4.12	0.60	4.57	1.45	31.2	26.8	6.6	10.4	0.15	3.86	10.7	16.4
Porac10		0.69	1.91	0.30	1.99	0.29	3.15	0.96	19.5	11.8	3.07	7.9	0.15	2.51	8.2	27.3
AC-BG1	Bundelkhand Gr.	0.26	0.76	0.11	0.98	0.16	2.86	1.04	29.6	19.4	4.19	10.7	0.13	0.92	5.7	61.5

The concentrations of the various elements, other than the rare earth elements (REE), are within 5% error. The REE, in particular Sm and Nd, are more precisely determined to within 2% error.

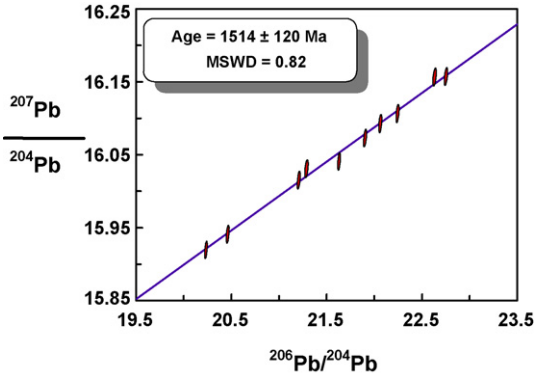

Fig. 3. Pb–Pb isotope ratio plots for the whole-rock limestones of the Rhotas Formation of the Semri Group, lower Vindhyans. The measured ratios show an isochron with a 1514 Ma age and an 120 Ma (2σ) error. This 1514 ± 120 Ma age is similar, within errors, to the Pb–Pb ages of the Rhotas limestone reported in two recent studies (Ray et al., 2003; Sarangi et al., 2004).

al., 2003) to 1599 ± 48 Ma (Sarangi et al., 2004). Our Pb–Pb age estimates of 1514 ± 120 Ma (2σ, MSWD 0.82) for the Rhotas Formation (Fig. 3, Table 2), as presented in this study, are in agreement with the above-mentioned ages. Pb–Pb ages of the Kajrahat Limestone from the Semri Group at the basal Vindhyans (Fig. 2) indicate that the initiation of sedimentation in the Vindhyan Basin took place earlier than 1721 Ma. (Sarangi et al., 2004; Ray, 2006).

Reliable radiometric age data for the upper Vindhyan rocks are lacking. This is mainly because of the challenges associated with the determination of absolute ages of sedimentary sequences using the common long-lived isotope systems like U–Pb, Sm–Nd and Rb–Sr. In particular, these isotopic signatures, inherited by the minerals in sedimentary rocks reflect characteristics of their source rocks and are often variably affected by diagenesis of the sediments. The Kaimur sandstones of the upper Vindhyan are intruded by the Majhgawan kimberlite, which was emplaced ~1075 Ma (Ar–Ar) ago indicating that while the depositional ages of the Rewa and Bhander Groups of upper Vindhyan are definitely younger than ~1075 Ma, the Kaimur sandstones were deposited prior to 1075 Ma (Gregory et al., 2006). Sr-isotope stratigraphy, which involves correlation of the Sr-isotopic composition of pristine limestones with the global seawater Sr isotope evolution curve indicates that the Bhander limestones of upper Vindhyan were deposited between 750 and 725 Ma (Ray et al., 2003). Based on the occurrence of *Diplocraterion* burrows from the Bhander sediments, it has been suggested that Vindhyan sedimentation might have continued till the Precambrian–Cambrian boundary (Chakrabarti, 1990).

Table 2
Pb isotopic compositions of 10 samples from the Rhotas Limestone

Sample#	$^{206}Pb/^{204}Pb$	$^{207}Pb/^{204}Pb$	$^{208}Pb/^{204}Pb$
VRH-2	22.752	16.157	41.515
VRH-1	22.246	16.107	40.890
VRH-5	20.475	15.943	39.817
VRH-4	21.296	16.032	40.521
VRH-3	21.906	16.074	40.952
VRH-2-2	22.632	16.157	41.457
VRH-1-2	21.635	16.042	40.409
VRH-5-2	20.247	15.922	39.627
VRH-4-2	21.215	16.017	40.546
VRH-3-2	22.066	16.093	41.111

As shown in Fig. 3 the Pb–Pb isochron yields an ages of 1514 ± 120 Ma for the Rhotas Limestone which is in agreement with previously reported ages of this lithounit (see text for discussion).

5. Results

5.1. Trace element geochemistry

Chondrite-normalized REE patterns for the Vindhyan Basin samples and the solitary Bundelkhand granite sample of the present study are shown in Fig. 4. All samples show overall uniform light-REE enriched patterns in chondrite-normalized plots with average $La/Yb_{(N)}$ values of 10.7 for the Bundelkhand granite, 11.7 for the Porcellanites and ranging from 5.6 to 10.9 for the remaining sedimentary rocks. All the rocks are also characterized by prominent negative Eu-anomalies, with average Eu-anomalies, $Eu/Eu^* = Eu/(Sm^*Gd)^{0.5}$, ranging from 0.81 for the granite, 0.41 for the porcellanites and ranging from 0.65 to 0.52 for the other rocks. REE concentrations for most of the clastic samples and the porcellanites are similar, except for the upper Rewa sandstones, which have concentrations one-quarter to one-third lower. The impure limestones from the Rhotas Formation in the lower Vindhyan and one sample of the Bhander Limestone from the upper Vindhyan also show distinctly lower REE concentrations.

Whole-rock multiple trace element data of the Vindhyan samples and the Bundelkhand granite are shown in Table 1. These trace element concentration data are also shown in Fig. 4 normalized over primitive mantle values with the elements arranged according to progressively decreasing incompatibility from the left to the right. The porcellanites are characterized by depletions in Ba, Nb, Ta, Sr and Eu. While some porcellanites show depletions in Pb, others show slight enrichments in Pb.

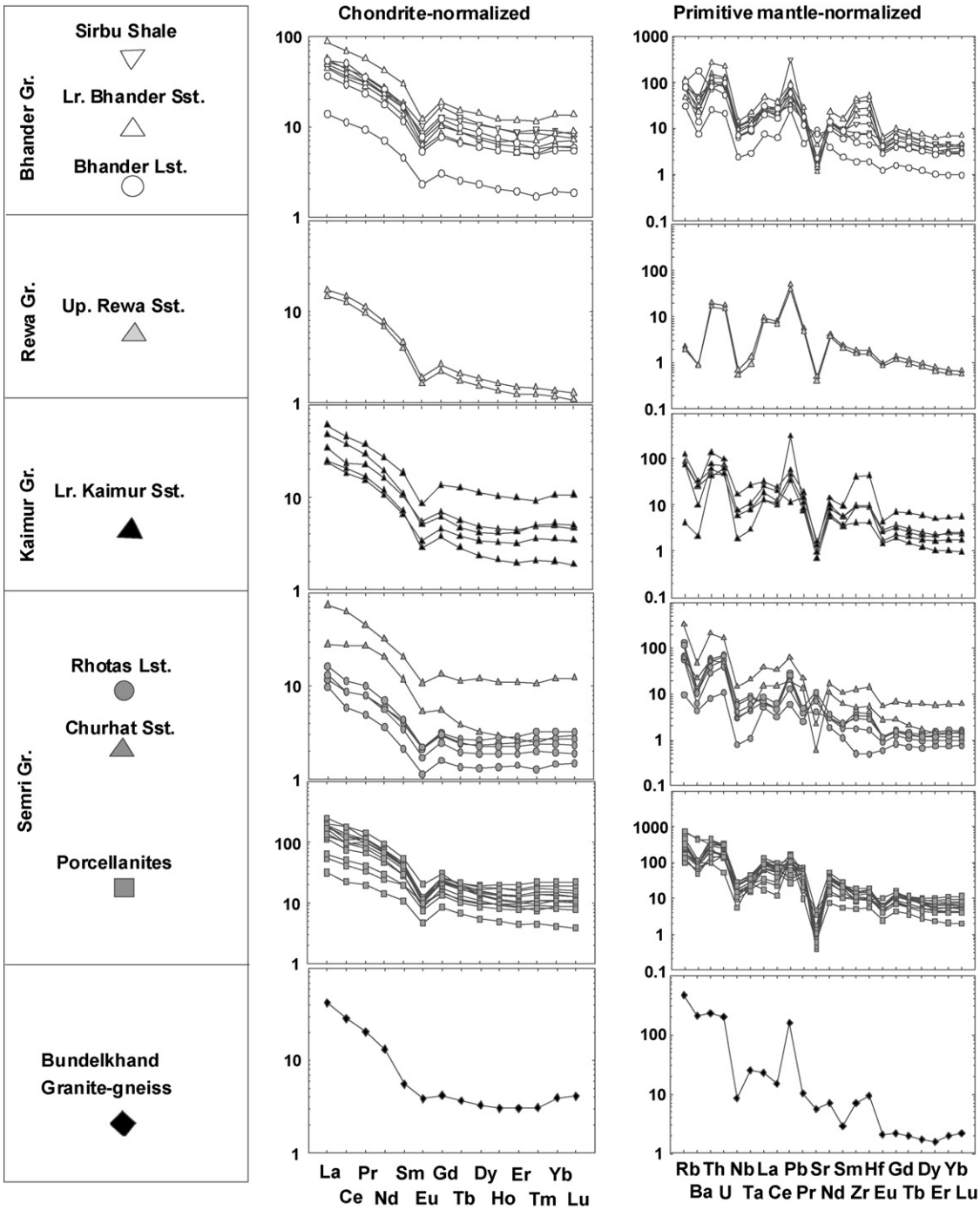

Fig. 4. Chondrite-normalized rare earth element (REE) patterns and primitive mantle-normalized compatible and incompatible element ratio plots for the Vindhyan Basin sediments, the Porcellanites and the Bundelkhand granite as analyzed in this study (Table 1). The trace element patterns of the Bundelkhand granite are remarkably different from those of the Vindhyan Basin samples. Trace element patterns of the porcellanites are similar to arc-derived rocks (also see Fig. 5). The Rewa Group of rocks with low trace element concentrations show different patterns, especially lower Rb, Zr and Hf, compared to the underlying Kaimur and overlying Bhander Group of rocks.

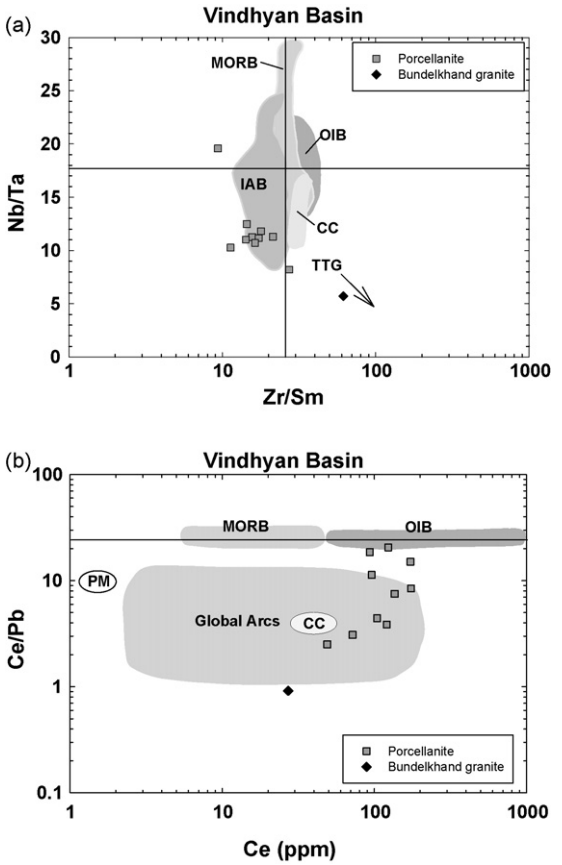

Fig. 5. Trace element ratios of the Porcellanites indicate that these volcanics were formed in a subduction zone setting. In a Nb/Ta vs. Zr/Sm plot (a), most of the porcellanite samples overlap with the field of island arc basalts while in a Ce/Pb vs. Ce plot (b), the porcellanites show a mixing trend between mantle-derived rocks and the average continental crust (CC) and overlap with the field of global arcs (Miller et al., 1994).

In contrast, most of the other sediments as well as the Bundelkhand granite show prominent Pb enrichments. The sedimentary rocks also show depletions in Ba, Nb, Ta, Sr, and except for the Rewa sandstones and a few limestone samples from the Rhotas and Bhander Formations, they all show enrichments in Zr and Hf similar to the Bundelkhand granite. The porcellanites however, do not show any Zr or Hf anomaly. Trace element ratios of the porcellanites also overlap with average present-day global arc rocks (Tatsumi and Eggins, 1995). In a Nb/Ta versus Zr/Sm plot (Foley et al., 2002) shown in Fig. 5a, most of the porcellanite samples overlap with the field of arc basalts while in a Ce/Pb versus Ce plot (Fig. 5b), the porcellanites show a mixing trend between mantle-derived rocks and the average continental crust and overlaps with the field of global arcs (Miller et al., 1994).

5.2. Sm–Nd systematics

Nd-isotopic compositions of all the lithounits of the foregoing discussion are reported in Table 3 and their present day Nd isotopic compositions are shown in Fig. 6. The present day Nd isotopic compositions of the Semri Group of rocks, including the porcellanites, overlap and range from −22.7 to −16.7. The Kaimur and Rewa rocks also have overlapping $\varepsilon_{Nd(0)}$ and range from −18.7 to −16.1 while those of the Bhander Group of rocks range from −16.9 to −13.8. Overall, the present day Nd-isotopic compositions of the Vindhyan rocks show progressively more radiogenic compositions with decreasing stratigraphic age. The solitary Bundelkhand granite sample shows very unradiogenic present-day $\varepsilon_{Nd(0)}$ of −34. The Nd isotopic ratios show an abrupt increase towards comparatively more radiogenic values at the boundary between the Semri and Kaimur Groups and between the Rewa and Bhander Group of rocks (Fig. 6). Initial ε_{Nd} of the porcellanites at 1630 Ma range from −5.7 to −0.9, while those of the two Churhat Sandstone samples at 1630 Ma are −6.7 and −4.3 and the Rhotas Limestone at 1600 Ma ranges from −10.3 to −6.2 (Table 3). Because of the lack of reliable radiometric age constraints for the deposition of the upper Vindhyan rocks, their initial Nd isotopic compositions cannot be estimated.

$f_{Sm/Nd}$, which is a measure of Sm and Nd fractionation with respect to bulk earth Sm/Nd, is −0.56 for the Bundelkhand granite while those of the porcellanites range from −0.42 to −0.31 (Table 3). The remaining Semri Group of rocks show overlapping $f_{Sm/Nd}$, which range from −0.41 to −0.27. There is no significant difference between the $f_{Sm/Nd}$ of the uppermost Semri Group of rocks and the Kaimur sandstones ($f_{Sm/Nd}$ = −0.41 to −0.29) although the Kaimur Group of rocks have comparatively more radiogenic Nd isotopic compositions. However, $f_{Sm/Nd}$ values abruptly increase at the boundary between the Rewa Group ($f_{Sm/Nd}$ = −0.38 to −0.39) and the Bhander Group (Fig. 6) with $f_{Sm/Nd}$ ranging from −0.34 to −0.32 for the Bhander Limestone, −0.33 to −0.26 for the lower Bhander Sandstone and −0.29 for the Sirbu Shale.

Depleted mantle Nd model age (T_{DM}), which indicates the time of extraction of the melt (source rock for sediments) from a depleted mantle source, is 2.7 Ga for the Bundelkhand granite, while those of the porcellanites range from 2.3 to 2.8 Ga (Table 3). The Semri Group of rocks show overlapping T_{DM} ages, with the Rhotas Limestone recording the oldest age of ∼3.2 Ga. There is an abrupt decrease in T_{DM} ages across the boundary between the lower and upper Vindhyan rocks with the

Table 3
Nd isotopic compositions of the Vindhyan Basin rocks. Also shown are their $f_{Sm/Nd}$ and depleted mantle model ages (T_{DM}). Initial ε_{Nd} are only reported for Porcellanites, Churhat sandstone, and Rhotas limestone, which have good radiometric age constraints on their time of deposition

Sample id	Description	$^{143}Nd/^{144}Nd$ (0)[a]	$^{147}Sm/^{144}Nd$	$f_{Sm/Nd}$[b]	$\varepsilon_{Nd(0)}$[c]	$\varepsilon_{Nd(T)}$[d]	T_{DM}[e] (Ga)
Sirbu-1	Sirbu Shale	0.511822	0.1400	−0.29	−15.9		2.7
LBS-1	Lr Bhander Sst	0.511769	0.1328	−0.33	−16.9		2.6
LBS-2		0.511887	0.1379	−0.30	−14.7		2.5
LBS-3		0.511847	0.1420	−0.28	−15.4		2.8
LBS-4		0.511799	0.1451	−0.26	−16.4		3.0
LBL-1	Bhander Lst	0.511845	0.1301	−0.34	−15.5		2.4
LBL-2		0.511933	0.1301	−0.34	−13.8		2.2
LBL-3		0.511823	0.1339	−0.32	−15.9		2.5
VR-1	Rewa Sst	0.511693	0.1217	−0.38	−18.4		2.4
VR-2		0.511755	0.1200	−0.39	−17.2		2.3
AC-KMS1	Kaimur Sst	0.511744	0.1397	−0.29	−17.4		2.9
VK-1		0.511812	0.1343	−0.32	−16.1		2.6
VK-2		0.511684	0.1263	−0.36	−18.6		2.5
VK-3		0.511682	0.1157	−0.41	−18.7		2.3
VK-3A		0.511744	0.1229	−0.38	−17.4		2.4
VRH-4	Rhotas Lst	0.511584	0.1430	−0.27	−20.6	−9.6	3.2
VRH-3		0.511510	0.1396	−0.29	−22.0	−10.3	3.2
VRH-1		0.511589	0.1267	−0.36	−20.5	−6.2	2.7
CHAC-2	Churhat Sst	0.511564	0.1169	−0.41	−20.9	−4.3	2.5
CHAC-1		0.511609	0.1325	−0.33	−20.1	−6.7	2.9
Porac1	Porcellanite	0.511784	0.1214	−0.38	−16.7	−0.9	2.3
Porac2		0.511677	0.1219	−0.38	−18.8	−3.1	2.4
Porac3		0.511522	0.1171	−0.41	−21.8	−5.2	2.6
Porac4		0.511507	0.1135	−0.42	−22.1	−4.7	2.5
Porac5		0.511509	0.1139	−0.42	−22.0	−4.8	2.5
Porac6		0.511660	0.1244	−0.37	−19.1	−4.0	2.5
Porac7		0.511577	0.1146	−0.42	−20.7	−3.6	2.4
Porac8		0.511477	0.1176	−0.40	−22.7	−6.2	2.6
Porac9		0.511589	0.1240	−0.37	−20.5	−5.3	2.6
Porac10		0.511691	0.1353	−0.31	−18.5	−5.7	2.8
AC-BG1	Bundelkhand Granite	0.510897	0.0865	−0.56	−34.0		2.7

[a] Measured $^{143}Nd/^{144}Nd$ ratios were normalized to $^{146}Nd/^{144}Nd = 0.7219$. Uncertainties for the $^{143}Nd/^{144}Nd$ ratios in the samples correspond to 2 in the fifth decimal place, representing 2σ of the mean. La Jolla Nd-standard analyzed during the course of this study yielded $^{143}Nd/^{144}Nd = 0.511852 \pm 24$ ($n = 3$).

[b] $f_{Sm/Nd}$ was calculated as $[(^{147}Sm/^{144}Nd)_{sample}/(^{147}Sm/^{144}Nd)_{CHUR} - 1]$ where CHUR is the chondritic uniform reservoir and $(^{147}Sm/^{144}Nd)_{CHUR}$ is 0.1967.

[c] $\varepsilon_{Nd}(0)$ was calculated using the present day bulk earth (CHUR) value of $^{143}Nd/^{144}Nd = 0.512638$ and $^{147}Sm/^{144}Nd = 0.1967$. The $\varepsilon_{Nd}(0)$ values represent the deviation of $^{143}Nd/^{144}Nd$ in parts per 10^4 from the present day CHUR value.

[d] Initial ε_{Nd} was determined only for samples for which radiometric age data are available.

[e] Depleted mantle Nd model ages (T_{DM}) were calculated using $\varepsilon_{Nd(0)} = +10$ and $^{147}Sm/^{144}Nd = 0.2136$ for the depleted mantle.

Kaimur Sandstone showing T_{DM} ages ranging from 2.3 to 2.9 Ga (Fig. 6). Unlike $\varepsilon_{Nd(0)}$ values, the T_{DM} ages do not change abruptly at the boundary between the Rewa and Bhander Groups. The lower Bhander Sandstone and Sirbu Shale units however, have older T_{DM} ages (2.5–3.1 Ga) compared to the Bhander Limestone ($T_{DM} = 2.2$–2.5 Ga).

6. Discussion

6.1. Genesis of the Porcellanites

The occurrence of porcellanites (silicified rhyolite tuffs) in the Semri Group indicates active volcanism during deposition of these rocks. The porcellanites are light

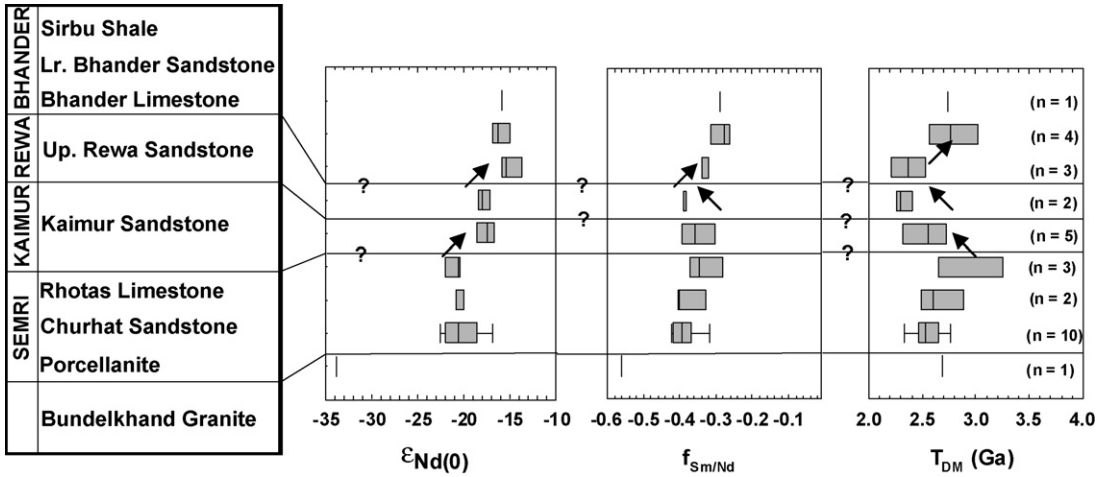

Fig. 6. Present day Nd isotopic compositions, plotted as $\varepsilon_{Nd(0)}$, of the Vindhyan Basin rocks and the Bundelkhand granite, as well as their $f_{Sm/Nd}$ and depleted mantle model ages (T_{DM}). The enrichment factor, $f_{Sm/Nd}$ is the deviation of $^{147}Sm/^{144}Nd$ of the sample from the chondritic uniform reservoir (CHUR) value. Overall, the Nd isotopic compositions of the Vindhyan rocks become progressively more radiogenic with decreasing stratigraphic age. There is also an abrupt increase in the Nd isotopic ratios across the boundaries between the Semri–Kaimur Groups and the Rewa–Bhander Groups. $f_{Sm/Nd}$ and T_{DM} ages change abruptly across the Kaimur–Rewa boundaries. The boundaries between the four groups of rocks in the Vindhyan Basin are characterized by change in provenance indicating that sedimentation in this basin was not continuous over ~1 Ga, punctuated by repeated tectonic activities.

green in color, massive and consist of a fine matrix of sericite and microcrystalline quartz with coarser crystals of plagioclase, K-feldspar, microcline and quartz along with glass shards and tiny prismatic zircons. U–Pb zircons ages indicate that these rocks crystallized ~1630 Ma ago (Rasmussen et al., 2002; Ray et al., 2002).

The porcellanites are characterized by REE concentrations greater than those of average upper crustal rocks (Taylor and McLennan, 1985). They show LILE enrichment with depletions in Nb and Ta in primitive mantle-normalized plots (Fig. 4) characteristic of arc rocks (e.g. Tatsumi and Eggins, 1995). Their trace element ratios are also similar to average global arcs suggesting that these rocks are products of subduction zone volcanism. In the Nb/Ta versus Zr/Sm discrimination diagram (Foley et al., 2002) shown in Fig. 5a, most of the porcellanite samples analyzed in this study overlap with the field of arc basalts with low Nb/Ta ratios. The solitary sample of Bundelkhand granite shows the lowest Nb/Ta similar to global Tonalite-Trondhjemite gneisses (TTG). The low Nb/Ta ratios of the porcellanites are consistent with melting of amphibolites in subduction zone environments (Foley et al., 2002). Similarly, in a Ce/Pb versus Ce plot (Fig. 5b), the porcellanites, with Ce/Pb ratios as high as 20.6, show a mixing trend between mantle-derived rocks and the continental crust and most of the samples overlap with the field of global arcs (Miller et al., 1994). However, these volcanics have a pronounced depletion in Eu, which suggests plagioclase removal from the source melt or its mixing with the continental crust. Initial ε_{Nd} at 1630 Ma of the porcellanites range from −5.7 to −0.9 (Table 3) and are similar to those observed in 'Andean-type' arcs (Rogers and Hawkesworth, 1989; Basu et al., 1990). Values close to zero indicate presence of a mantle component in the source of these rocks while the wide scatter in their Nd-isotopic composition can be explained by shallow assimilation of varying amounts of granitic basement rocks. The average depleted mantle model age (T_{DM}) of the porcellanites, which represents the time of extraction of the porcellanite melt from depleted mantle source is 2.5 Ga.

6.2. Provenance of Vindhyan sediments

Heavy mineral studies suggest that the main provenance of the lower Vindhyan sediments is the 2.5 Ga old Bundelkhand granite (Tandon et al., 1991). However, the trace element and Nd isotopic composition of the solitary sample of the Bundelkhand granite analyzed in this study is distinctly different from those of the lower and upper Vindhyan sediments as well as the porcellanites (Figs. 4 and 6). This observation rules out the Bundelkhand granite as a potential sediment source for the Son valley Vindhyans. This inference, although based on one sample of this granite-gneiss, is considered to be robust because there is a large difference in the Nd-isotopic composition of this granite ($\varepsilon_{Nd(0)} = -34$) and the Son

Valley Vindhyan sediments (Fig. 6). Even if we allow the Bundelkhand granite-gneiss to have a large range in ε_{Nd} values, say 10 epsilon units, the difference still persists. In contrast, the trace element patterns of most of the sedimentary units, specifically the lower Vindhyan rocks, are broadly similar to those of the tuffs from the Porcellanite Formation suggesting that the arc that produced the porcellanites might have contributed sediments to the lower Vindhyan Basin.

In a sedimentary sequence, a decrease in T_{DM} or an increase in ε_{Nd} corresponds to an increased contribution of radiogenic Nd to the sediment. This increase may result from an addition of juvenile material or from termination of old crustal input. Addition of juvenile sediments is associated with tectonic activity, in the form of crustal uplift or renewed volcanism (Andersen and Samson, 1995). Archean and early to mid-Proterozoic sediments have depleted mantle Nd model ages that are close to their stratigraphic age, while those of younger sediments are much higher, by as much as 2.0 Ga, than their stratigraphic age (O'Nions et al., 1983).

Present day Nd-isotopic compositions of the Semri Group of rocks including the Porcellanite Formation, Churhat Sandstone and the Rhotas Limestone overlap with each other (Fig. 6). However, the average T_{DM} of the Rhotas Limestone (3.0 Ga) is higher than that of the Churhat Sandstone (2.7 Ga), the Porcellanite Formation (2.5 Ga) or even the Bundelkhand granite (2.7 Ga). Initial ε_{Nd} of the porcellanites at 1630 Ma range from −5.7 to −0.9, while those of the Churhat Sandstone at 1630 Ma range from −6.7 to −4.3 and the Rhotas Limestone at 1600 Ma from −10.3 to −6.2 (Table 3). Limestones from the Rhotas Formation, which are rhythmites of limestones and shales, have much older T_{DM} ages and unradiogenic Nd isotopic compositions compared to the other rocks of the Semri Group suggesting sediment contribution from an even older crustal source. However, their low trace element concentrations are typical of marine carbonates. The Churhat sandstones with Nd isotopic compositions similar to the porcellanites are possibly sediments derived from the arc which produced the tuffs.

The Nd isotopic ratios show an abrupt increase towards comparatively more radiogenic values across the boundary between the Semri and Kaimur Groups (Fig. 6). However, the $f_{Sm/Nd}$ values are almost identical across the boundary between these two groups indicating that the Nd isotopic compositions of these rocks are characteristic of the source rocks for these sediments and not an artifact of post-depositional diagenetic enrichment of Sm. There is also an abrupt decrease in the T_{DM} across the Semri–Kaimur boundary with average T_{DM} of the Kaimur Sandstone being 2.5 Ga compared to 3.0 Ga for the Rhotas Limestone (Fig. 6). The Nd-isotopic data indicate that there was a change in the provenance of the Vindhyan sediments across the Semri–Kaimur boundary with the Kaimur Group sediments being derived from more juvenile sources. The occurrence of a prominent angular unconformity at the boundary of the Semri and Kaimur Groups observed in parts of the Son valley Vindhyans (Chakraborty, 2006) supports our above statement. This isotopic as well as lithostratigraphic boundary between the Semri and Kaimur Groups possibly indicates a period of active tectonism and a hiatus in sedimentation in the Vindhyan Basin followed by a change of provenance for the Kaimur sediments. While the age of sedimentation of the Kaimur sediments is not well constrained, the intrusion of the Majhgawan kimberlites into the Kaimur Sandstone indicates that these sediments must have been older than 1073 Ma, which is the age of emplacement of the kimberlite (Gregory et al., 2006).

The Kaimur and Rewa sandstones analyzed in this study have overlapping present day Nd isotopic compositions (Fig. 6). However, the average T_{DM} of the Rewa Sandstone (2.3 Ga) is younger than those of the underlying Kaimur Sandstone (2.5 Ga). The Rewa sandstones also have a lower $f_{Sm/Nd}$ compared to the Kaimur sandstones, which over time could result in similar present day Nd isotopic compositions. The Rewa sandstones also show strikingly low trace element concentrations and higher $La/Yb_{(N)}$ ratios (average 10.9) compared to the Kaimur sediments (average $La/Yb_{(N)} = 8.2$). In addition, the Rewa sandstones do not show Zr, Hf enrichments like the Kaimur sandstones and have much lower Rb concentrations, lower than all other rocks of the Vindhyan Basin analyzed in this study. The distinctly different trace element patterns of the Kaimur and Rewa Group of rocks, and the younger T_{DM} ages of the Rewa Sandstone suggests different provenances for these two groups of rocks with sediments being derived from more juvenile sources for the Rewa Group. The sudden change in provenance was possibly related to tectonism in the basin and an associated break in sedimentation. Presence of angular unconformity between the uppermost unit of the Kaimur Group and the lowermost unit of the Rewa Group further attests our conclusions (Chakraborty, 2006).

The Bhander Group of rocks have much higher trace element concentrations than the underlying Rewa Sandstone (Fig. 4). In addition, the Bhander Limestone (average $La/Yb_{(N)} = 7.7$), lower Bhander Sandstone (average $La/Yb_{(N)} = 7.0$) and the Sirbu Shale (average $La/Yb_{(N)} = 5.9$), all belonging to the Bhander Group show less fractionated REE patterns compared

to the underlying Rewa Group of rocks (average $La/Yb_{(N)} = 10.9$). Most of the Bhander Group of rocks also show prominent enrichments in Zr and Hf and have much higher Rb concentrations compared to the Kaimur Group of rocks (Fig. 4). There is an abrupt increase in $f_{Sm/Nd}$ and Nd isotopic ratios towards comparatively more radiogenic values across the boundary between the Rewa and Bhander Group of rocks suggesting a change in provenance towards even more juvenile sources for the Bhander sediments (Fig. 6). This implies that at the boundary between the Rewa and Bhander Groups, there was renewed tectonism in the Vindhyan Basin and also possibly a gap in sedimentation, which is supported by the occurrence of angular unconformities between the Rewa and Bhander Groups in the southern part of the Vindhyan Basin (Chakraborty, 2006). However, the T_{DM} ages of the Rewa Sandstone (average 2.3 Ga) and the Bhander Limestone (average 2.4 Ga) show a strong overlap, suggesting that the sediment sources for the Rewa and Bhander Group rocks, though isotopically distinct, evolved from the depleted mantle at around the same time with different Sm/Nd ratios. Within the Bhander Group, the stratigraphically younger lower Bhander Sandstone and the Sirbu Shale were derived from older sources as indicated by their progressively unradiogenic Nd isotopic compositions and older T_{DM} ages (average 2.8 Ga and 2.7 Ga, respectively).

Our trace element and Nd isotopic data suggest that sedimentation in the Vindhyan Basin was not continuous. The boundaries between each of the four groups are characterized by tectonism and resultant change in provenance with sediments of the immediately overlying units being derived from comparatively more juvenile sources. These boundaries are also characterized by the occurrences of angular unconformities, which indicate gaps in sedimentation. Our data also provide constraints on the source of the Vindhyan sediments. It is clear that the Bundelkhand granite was not a major source of sediments for the Vindhyans. We argue that the arc that produced the porcellanites may have been the source of sediments for the lower Vindhyan units. Paleocurrent directions in the Vindhyan sediments are mostly northerly (Banerjee, 1974; Prasad, 1984) suggesting that the evolving Satpura orogen might have served as the source for the Vindhyan Basin sediments (Chakraborty, 2006). However, due to lack of isotopic and trace element data from the Satpuras, this hypothesis cannot be tested for sure. Recent geophysical studies (Mishra et al., 2002) across the Satpuras suggest that the Satpura fold belt represents a Proterozoic collisional zone between the Bundelkhand craton towards the north and Bhandara craton to its south. There is also plausible geophysical

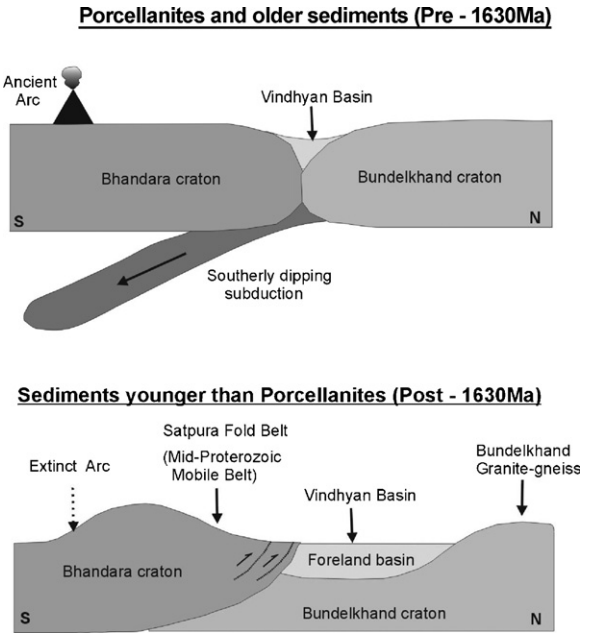

Fig. 7. Tectonic model showing initiation of sedimentation in the Vindhyan Basin. Collision of the Bundelkhand craton occurring to the north and the Bhandara craton situated to the south of the Vindhyan Basin, as seen today, was preceded by a southerly dipping subduction zone resulting in Andean-type arc magmatism. The Vindhyan Basin was possibly initiated as a Foreland Basin and sediments in the lowermost Vindhyans including the porcellanites were primarily derived from this now-extinct arc.

evidence of a southerly dipping subduction system south of the Satpuras (Mishra et al., 2002). We suspect that this subduction system, now extinct, might have supplied sediments to the Vindhyan Basin, which was possibly initiated as a foreland Basin upon collision between the Bundelkhand craton in the north and the Bhandara craton to the south. The above-mentioned tectonic model for the initiation of the Vindhyan Basin is shown in Fig. 7.

7. Conclusions

(1) Trace elements concentration data as well as Nd isotopic compositions of the 1.6 Ga old porcellanites from the Semri Group of the lower Vindhyans indicate that they were derived from an 'Andean-type' continental margin arc. The Nd isotopic compositions of these volcanic tuffs indicate their derivation from a mantle source accompanied by shallow assimilation of varying amounts of granitic basement rocks.

(2) Trace element concentration patterns as well as Nd isotopic compositions of the Vindhyan Basin sediments from the Son valley are vastly different from those of the Bundelkhand granite suggesting that

these granitic rocks were not a major source of sediments for the Vindhyan Basin.

(3) Sedimentation in the Vindhyan Basin lasted over ~1 Ga but was not continuous. The boundaries between the Semri and Kaimur Groups as well as the Rewa and Bhander Groups are characterized by abrupt changes in the Nd isotopic compositions with the Kaimur and Bhander Groups having more radiogenic Nd isotopic compositions compared to the Semri and Rewa Groups, respectively. This indicates changes in provenance with sediments in the Kaimur and Bhander Groups being derived from more juvenile sources compared to the Semri and Rewa Groups, respectively. This is also supported by changes in T_{DM} and $f_{Sm/Nd}$ across these boundaries. The strikingly different trace element patterns of the Rewa Group of sediments compared to the underlying Kaimur sediments indicates that sediment sources also changed across the Kaimur–Rewa boundary.

(4) While the exact source of sediments for the Vindhyan Basin remains unclear, we argue that the majority of the sediments, most certainly the lower Vindhyans, were derived from a now-extinct Andean-type arc occurring farther south resulting from a southerly dipping subduction before the collision of the Bhandara and Bundelkhand cratons. The Vindhyan Basin was initiated as a foreland Basin after collision of these two cratons.

Acknowledgements

This research was partially supported by NSF grants to ARB and a GSA student travel grant to RC.

References

Andersen, C.B., Samson, S.D., 1995. Temporal changes in Nd isotopic composition of sedimentary rocks in the Sevier and Taconic foreland basins: increasing influence of juvenile sources. Geology 23 (11), 983–986.

Banerjee, I., 1974. Barrier coastline sedimentation model and the Vindhyan example. Contributions to the Earth and Planetary Sciences Golden Jubilee Volume Quart. J. Geol. Min. Met. Soc. India 46, 101–127.

Basu, A.R., Sharma, M., DeCelles, P.G., 1990. Nd, Sr-isotopic provenance and trace element geochemistry of Amazonian Foreland Basin Fluvial Sands, Bolivia and Peru: implications for Ensialic Andean Orogeny. Earth Planet. Sci. Lett. 105, 149–169.

Bhattacharyya, A., 1996. Recent advances in Vindhyan Geology, vol. 36. Geological Society of India Memoir, p. 331.

Chakrabarti, A., 1990. Traces and dubiotraces: examples from the so-called Late Proterozoic siliciclastic rocks of the Vindhyan Supergroup around Maihar, India. Precambrian Res. 47, 141–153.

Chakrabarti, R., Abanda, P.A., Hannigan, R.E., Basu, A.R., 2007. Effects of diagenesis on the Nd-isotopic composition of Black Shales from the 420 Ma Utica Shale Magnafacies, Chem. Geol., in press.

Chakraborty, C., 2006. Proterozoic intracontinental basin: the Vindhyan example. J. Earth Syst. Sci. 115 (1), 3–22.

Chakraborty, P.P., Banerjee, S., Das, N., Sarkar, S., Bose, P.K., 1996. Volcaniclastics and their sedimentological bearing in Proterozoic Kaimur and Rewa Groups in central India, Memoir Geological Society of India, pp. 59–75.

Crawford, A.R., Compston, 1970. The age of Vindhyan system of peninsular India. Quat. J. Geol. Soc. Lond. 125, 351–371.

Das, L.K., Mishra, D.C., Ghosh, D., Banerjee, B., 1990. Geomorphotectonics of the basement in a part of upper Son Valley of the Vindhyan Basin. J. Geol. Soc. India 35 (5), 445–458.

Foley, S., Tiepolo, M., Vannucci, R., 2002. Growth of early continental crust controlled by melting of amphibolite in subduction zones. Nature 417, 837–840.

Gleason, J.D., Patchett, P.J., Ruiz, W.R.D., 1994. Nd isotopes link Ouachita turbidites to Appalachian sources. Geology 22, 347–350.

Gregory, L.C., et al., 2006. A paleomagnetic and geochronologic study of the Majhgawan kimberlite, India. Implications for the age of the upper Vindhyan Supergroup. Precambrian Res. 149, 65–75.

Hannigan, R.E., Basu, A.R., 1998. Late diagenetic trace element remobilization in organic-Rich Black Shales of the Taconic Foreland Basin of Quebec, Ontario and New York. In: Jurgen Schieber, W.Z., Sethi, Parvinder S. (Eds.), Shales and Mudstones II, pp. 209–233.

Kaila, K.L., Murty, P.R.K., Mall, D.M., 1989. The evolution of the Vindhyan Basin vis-a-vis the Narmada-Son Lineament, central India, from deep seismic soundings. Tectonophysics 162 (3/4), 277–289.

Krishnan, M.S., 1968. Geology of India and Burma. Tata McGraw Hill Publication, New Delhi.

Miller, R.G., O'Nions, R.K., 1984. The provenance and crustal residence ages of British sediments in relation to palaeogeographic reconstructions. Earth Planet. Sci. Lett. 68, 459–470.

Miller, D.M., Goldstein, S.L., Langmuir, C.H., 1994. Cerium/lead and lead isotope ratios in arc magmas and the enrichment of lead in the continents. Nature 368, 514–520.

Mishra, D.C., Singh, B., Gupta, S.B., 2002. Gravity modelling across Satpura and Godavari Proterozoic belts: geophysical signatures of Proterozoic collision zones. Curr. Sci. 83 (8), 1025–1031.

Mondal, M.E.A., Goswami, J.N., Deomurari, M.P., Sharma, K.K., 2002. Ionprobe $^{207}Pb/^{206}Pb$ ages of zircons from the Bundelkhand massif, northern India: implications for crustal evolution of the Bundelkhand-Aravalli protocontinent. Precambrian Res. 117, 85–100.

Naqvi, S.M., Rogers, J.J.W., 1987. Precambrian Geology of India. Oxford University Press, Oxford, 223 pp.

Nelson, B.K., DePaolo, D.J., 1988. Application of Sm–Nd and Rb–Sr isotope systematics to studies of provenance and basin analysis. J. Sediment. Petrol. 58, 348–357.

O'Nions, R.K., Hamilton, P.J., Hooker, P.J., 1983. A Nd isotope investigation of sediments related to crustal development in the British Isles. Earth Planet. Sci. Lett. 63, 229–240.

Prasad, B., 1984. Geology, sedimentation and paleogeography of the Vindhyan Supergroup, S.W. Rajasthan. Mem. Geol. Surv. India 116 (1), 1–107.

Rasmussen, B., et al., 2002. 1.6 Ga U–Pb zircon age for the Chorhat Sandstone, lower Vindhyan, India: possible implications for early evolution of animals. Geology 30 (2), 103–106.

Ray, J.S., 2006. Age of the Vindhyan Supergroup: a review of recent findings. J. Earth Syst. Sci. 115 (1), 149–160.

Ray, J.S., Martin, M.W., Veizer, J., Bowring, S.A., 2002. U–Pb zircon dating and Sr isotope systematics of the Vindhyan Supergroup, India. Geology 30 (2), 131–134.

Ray, J.S., Veizer, J., Davis, W.J., 2003. C, O, Sr, and Pb isotope systematics of carbonate sequences of the Vindhyan Supergroup, India: age, diagenesis, correlations and implications for global events. Precambrian Res. 121, 103–140.

Rogers, J.J.W., 1986. The Dharwar craton and the assembly of Peninsular India. J. Geol. 94, 129–143.

Rogers, G., Hawkesworth, C.J., 1989. A geochemical traverse across the North Chilean Andes: evidence for crust generation from the mantle wedge. Earth Planet. Sci. Lett. 91, 271–285.

Roy, A.B., 1988. Stratigraphic and tectonic framework of the Aravalli mountain range. In: Roy, A.B. (Ed.), Precambrian of the Aravalli Mountain. India Memoir—Geological Society of India, Rajasthan, pp. 3–31.

Roy, A., Bandyopadhyay, B.K., 1990. Cleavage development in Mahakoshal Group of rocks of Sleemanabad-Sihora area, Jabalpur District, Madhya Pradesh. Indian Miner. 44 (2–3), 111–128.

Sarangi, S., Gopalan, K., Kumar, S., 2004. Pb–Pb age of earliest megascopic, eukaryotic alga bearing Rhotas Formation, Vindhyan Supergroup, India: implications for Precambrian atmospheric oxygen evolution. Precambrian Res. 132, 107–121.

Seilacher, A., Bose, P.K., Pfluger, F., 1998. Triploblastic animals more than 1 Billion years ago: trace fossil evidence from India. Science 282, 80–83.

Sharma, M., Basu, A.R., Nesterenko, G.V., 1992. Temporal Sr, Nd and Pb isotopic variations in the Siberian flood basalts: implications for the plume-source characteristics. Earth Planetary Sci. Lett. 113, 365–381.

Simien, F., Mattauer, M., Alegre, C.J., 1999. Nd isotopes in the Stratigraphic record of the Montagne Noire (French Massif Central): no significant Paleozoic Juvenile inputs, and Pre-Hercynian Paleogeography. J. Geol. 107, 87–97.

Tandon, S.K., Pant, C.C., Casshyap, S.M., 1991. Sedimentary basins of India—Tectonic context. Gyanodaya Prakashan, Nainital.

Tatsumi, Y., Eggins, S., 1995. Subduction Zone Magmatism. Frontiers in Earth Sciences. Blackwell Science, 211 pp.

Taylor, S.R., McLennan, S.M., 1985. The Continental Crust: its Composition and Evolution. Blackwell scientific publications, 312 pp.

Tewari, A.P., 1968. A new concept of paleotectonic setup of a part of a part of northern peninsular India with special reference to the great boundary faults. Geol. Mijnbouw 47, 21–27.

Verma, R.K., 1991. Geodynamics of the Indian Peninsula and the Indian Plate Margin. IBH, Oxford, 357 pp.